A three dimensional numerical study of rotating buoyant convection in a side heated cavity

A. MEDELFEF[a,b], D. HENRY[b], A. BOUABDALLAH[a], R. BOUSSAA[a], S. KADDECHE[c] and V. BOTTON[b,d]

a. Laboratoire de Thermodynamique et Systèmes Energétiques, Faculté de Physique, Université des Sciences et de la Technologie Houari Boumediene, BP 32, El Alia 16111, Bab Ezzouar, Algérie. E-mail : abs.medelfef@gmail.com

b. Laboratoire de Mécanique des Fluides et d'Acoustique, CNRS/Université de Lyon, Ecole Centrale de Lyon/Université de Lyon 1/INSA de Lyon, ECL - 36 Av Guy de Collongue 69134 Ecully cedex, France. E-mail : daniel.henry@ec-lyon.fr

c. Laboratoire de Recherche Matériaux, Mesures et Applications, Institut National des Sciences Appliquées et de Technologie, Université de Carthage, BP 676, 1080 Tunis Cedex, Tunisie. E-mail : slimkaddeche@yahoo.fr

d. INSA Euro-Méditerranée, Université Euro-Méditerranéenne de Fès, Route de Meknès, BP 51, 30000 Fès, Maroc. E-Mail : valery.botton@insa-lyon.fr

Résumé :

L'objectif de ce travail est d'examiner l'effet de la rotation sur l'écoulement généré par un gradient de température horizontal dans une cavité tridimensionnelle. La rotation, par l'action de la force de Coriolis, induit une diminution considérable de l'amplitude de vitesse de l'écoulement cellulaire initial avec un renforcement de la vitesse transversale initialement faible. L'écoulement se trouve ainsi dévié vers la droite de la composante de vitesse dominante, ce qui engendre une modification cruciale de sa structure. L'écoulement évolue ainsi d'une boucle longitudinale unique vers une structure asymptotique complexe constituée de deux rouleaux longitudinaux concentrés près des parois latérales, qui sont mutuellement alimentés par un rouleau transverse dans toute la région de coeur. Dans les régions de montée ou de descente du fluide aux extrémités, la rotation favorise l'écoulement à travers la boucle longitudinale qui se situe à droite quand l'écoulement s'approche de la paroi considérée. Enfin, un modèle monodimensionnel simplifié, valable uniquement dans le noyau de la cavité, est dérivé et comparé aux résultats numériques.

Abstract:

The aim of this work is to examine the effect of the rotation on the flow generated by a horizontal temperature gradient in a three-dimensional cavity. The rotation, through the action of the Coriolis force, induces a decrease of the main longitudinal flow, with a concomitant increase of the originally weak transverse velocity. This effect is particularly pronounced in the core of the cavity, which was the original region of main flow. As a result, the overall flow structure is changed. The initial well symmetric single roll flow is first deviated towards a diagonal of the cavity, with only the central symmetry kept. At larger rotation rates, in an asymptotic domain where all the velocity components eventually decrease, the

longitudinal circulation is maintained in two rolls along the front and back lateral walls, while mainly transverse transfers occur in the core between these rolls. Finally, a 1D simplified model which is valid only in the core of the cavity is derived and compared with the numerical results.

Keywords : natural convection, rotating flow, heated flow, Taylor number.

1 Introduction

Heated flows have aroused the interest of physicists for a long time because of their implication in various fundamental and engineering fields such as astrophysics, geophysics, cooling processes of nuclear reactors, electronics or even the human body. One of the problems encountered in the crystal growth using the horizontal Bridgman method (it consists in pulling the melt in a horizontal temperature gradient) is the appearance of striations in the solid which are nothing else than a recording of hydrodynamic instabilities developing in the melt and gradually attached in the solid as the solidification front advances [1]. The appearance and the nature of these instabilities depend on several parameters such as the nature of the materials (Prandtl number) [2, 3], the container and even the boundary conditions [4, 5].

At a larger scale, buoyant convection insures the atmospheric circulation of air like the trade winds which are known as the Hadley circulation [6]. Side-heated convection has been experimentally investigated in order to mimic this situation by Fultz [7] and by Hide [8, 19]. These experiments were carried out in a fluid confined between two co-axial cylinders subjected to a radial horizontal temperature gradient. In addition to the horizontal temperature gradient, Hide [8, 19] added the effect of the Coriolis force by setting its experiment in a rotating table.

Side-heated convection has been widely studied in the past. Experimental and numerical studies of the flow in differentially heated rectangular cavities and its first transitions were performed. See, for example, Hurle et al. [10], Hof et al. [11], Ben Hadid et al. [12, 13], Henry et al. [2, 14], Xu et al. [15] and Dridi et al. [16]. In these studies, the effects of the fluid nature (Prandtl number), the cavity dimensions, the acoustic streaming and the magnetic field (as well as its directional effect) were investigated in order to control the flow and its transition to oscillatory convection. However, the effect of rotation on the convection in a side heated rectangular cavity has never been discussed in the literature, despite its interest in many situations.

2 Mathematical model and symmetries of the problem

We consider the flow in a cavity of aspect ratios $A_X = L/h = 4$ and $A_Z = l/h = 2$ where L is the length along the longitudinal x-direction, h is the height along the vertical y-direction, and l is the width along the transverse z-direction. This cavity is heated from the side ans is submitted to a rotation around the vertical y-axis (Fig.1). The Boussinesq approximation is used to describe the density evolution in the buoyancy term.

By using h, h^2/ν, ν/h, $\rho_0\nu^2/h^2$ and $\Delta T/A_X$ as reference quantities for length, time, velocity, pressure and temperature, the dimensionless equations of momentum, mass and energy become:

$$\partial_t \vec{V} + \vec{V}.\vec{\nabla}\vec{V} = -\vec{\nabla}p + \nabla^2\vec{V} + Gr\,\Theta\,\vec{e}_y + \sqrt{Ta}\,(\vec{V}\times\vec{e}_y), \tag{1}$$

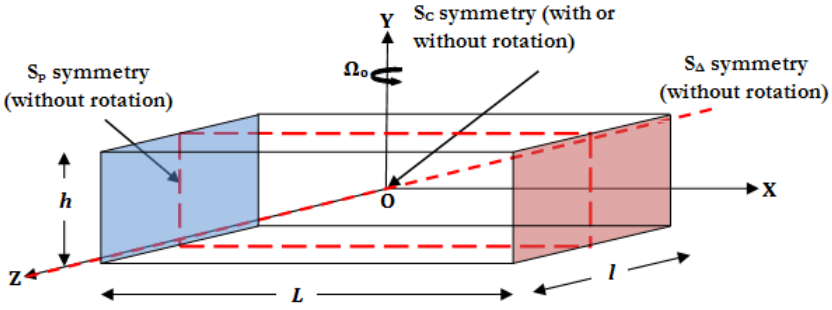

FIGURE 1 – Geometry and symmetries of the problem.

$$\partial_t \Theta + \vec{V}.\vec{\nabla}\Theta = Pr^{-1}\nabla^2\Theta, \tag{2}$$

$$\vec{\nabla}.\vec{V} = 0, \tag{3}$$

where $Ta = 4\Omega_0^2 h^4/\nu^2$ is the Taylor number, $Gr = g\beta h^3 \Delta T/\nu^2$ is the Grashof number and $Pr = \nu/\alpha$ is the Prandtl number.

The boundary conditions are the no-slip conditions for the velocity $U = V = W = 0$ at the walls and $\vec{\nabla}\Theta.\vec{n} = 0$ for insulating lateral walls (at $y = \pm 1/2$ and $z = \pm A_Z/2$) and $\Theta(x = \pm A_X/2) = \pm A_X/2$ for the isothermal walls.

These boundary conditions and geometry impose some symmetries, which can be broken or kept in a given situation (rotating or static cavity for example). It is therefore important to determine them before doing the simulations. By analyzing the geometry given in Fig. 1, we can determine the following symmetries in the case without rotation:

— Symmetry with respect to the z-axis, S_Δ (π rotation):

$$S_\Delta : (x, y, z, t) \rightarrow (-x, -y, z, t)\ ,\ (U, V, W, \Theta) \rightarrow (-U, -V, W, -\Theta)$$

— Symmetry with respect to the vertical middle plane perpendicular to the z-axis, S_P:

$$S_P : (x, y, z, t) \rightarrow (x, y, -z, t)\ ,\ (U, V, W, \Theta) \rightarrow (U, V, -W, \Theta)$$

— Symmetry with respect to the center of the cavity as a resulting global symmetry, S_C such that:

$$S_C = S_\Delta.S_P$$

This S_C symmetry is the only symmetry that remains in the case with rotation.

Equations (1), (2) and (3) are solved using a spectral element code developed by Ben Hadid and Henry [13]. Spatial discretization is achieved by Gauss-Lobatto-Legendre polynomials while time discretization is carried out by a semi-implicit scheme proposed by Karniadakis [17] where the nonlinear terms are included explicitly while the linear terms are solved implicitly and finally, the pressure is determined by imposing the incompressibility constraint. For more details on the code, see El Gallaf [18].

3 Results and discussions

The numerical simulations of the steady state flow were carried out for Taylor numbers ranging from 0 to 10^6, while the Grashof and the Prandtl number have been fixed at 2.5×10^4 and 10^{-3} respectively.

3.1 Flow structure

The laminar buoyant convection obtained before the onset of the first instability in the absence of rotation ($Ta = 0$) is a one cell flow occupying the entire enclosure, in which the flow rises at the hot side boundary, moves toward the cold wall and then descends along it to finally reach the hot wall again. However, it is known that in the case of extended cavities, the flow undergoes the development of rolls inside the long cell flow due to a shear instability [4]. Because of the flow confinement in our parallelepipedic cavity, this transition has become an imperfect bifurcation [5] and its effect appears as a bump in the vertical velocity profile $V(x)$ at $x \approx \pm 0.7$ (Fig. 2a).

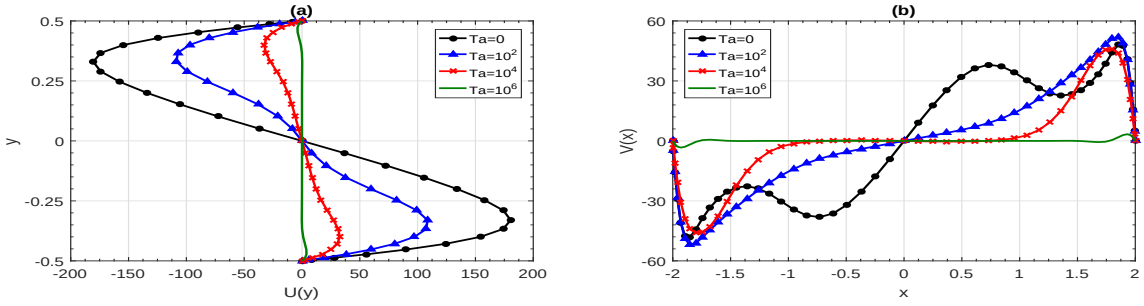

FIGURE 2 – Effect of the Taylor number on: (a) the longitudinal velocity profile $U(y)$ at $x = z = 0$ and (b) the vertical velocity profile $V(x)$ at $y = z = 0$ for $Pr = 10^{-3}$ and $Gr = 2.5 \times 10^4$.

When we introduce the rotation, the dynamics of the flow is affected by the Coriolis force. It does not act as a forcing of the flow (as it preserves the case of rest when the Grashof number is zero), but as a correction, acting on the components of the velocity initially induced by differentially heating the sidewalls. With the rotation chosen here (see Fig. 1) the flow is thus diverted to the right for the dominant longitudinal component of the velocity, creating transverse velocities while maintaining the symmetry S_C with respect to the center. This deviation of the flow causes great changes in the structure of the convective flow, greatly reducing the velocity amplitude (Figs. 2 and 3) and modifying the original single loop to a more complex structure with transverse velocities, which will be exhibited in the next paragraph.

More detailed information on the structure of the flow is now given by velocity contours in transverse planes (Fig. 3). The choice of this plane to represent the velocity contours is motivated by the fact that this plane illustrates the flow symmetries. In the case without rotation ($Ta = 0$), the contours of the longitudinal component of the velocity $U(y, z)$ in the central transverse plane at $x = 0$ show clearly the existence of a single convective cell within the flow and reflect the symmetries S_Δ, S_P and S_C (Fig. 3a). When the cavity is set in rotation ($Ta > 0$), the symmetries S_Δ and S_P are broken and the convective cell undergoes substantial changes resulting from the deviation of the flow due to the rotation (Figs. 3b, 3c and 3d). The longitudinal velocity component becomes more concentrated in two corners, the upper corner at $z = -1$ and the lower corner at $z = 1$ (Figs. 3b and 3c). When the Taylor number is sufficiently increased, maxima of the longitudinal velocity also appear in the two other corners. Finally, at large Taylor numbers ($Ta = 10^6$), an asymptotic state structure with almost symmetric maxima of

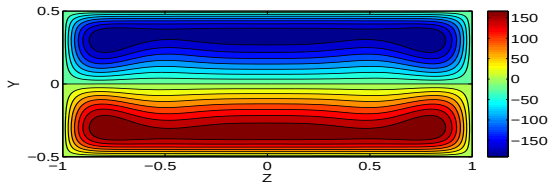

(a) $Ta = 0$

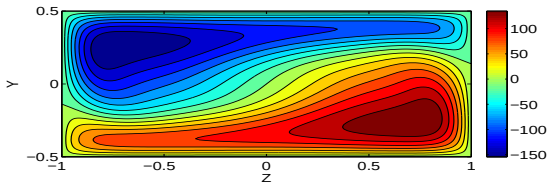

(b) $Ta = 10^2$

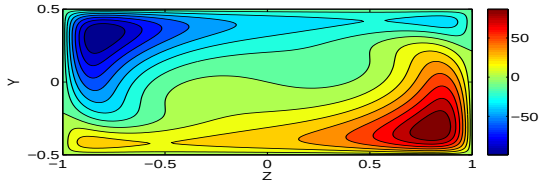

(c) $Ta = 10^4$

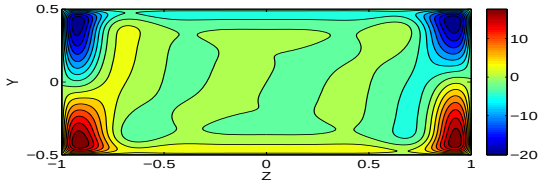

(d) $Ta = 10^6$

FIGURE 3 – Longitudinal velocity contours $U(y, z)$ at $x = 0$ for different Taylor numbers for $Pr = 10^{-3}$ and $Gr = 2.5 \times 10^4$.

the longitudinal velocity in the four corners is obtained (Fig. 3d). It was observed that the evolution towards this asymptotic state is delayed to larger values of the Taylor number when the Grashof number is increased. It seems that the inertia acquired by the flow when the Grashof number is large makes the deviation of the flow by the rotation, and thus the structural changes more difficult.

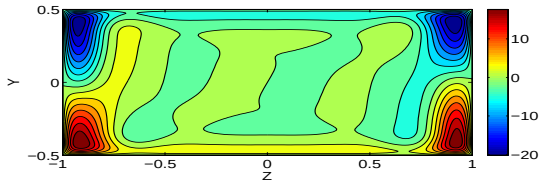

(a) $U(y, z)$

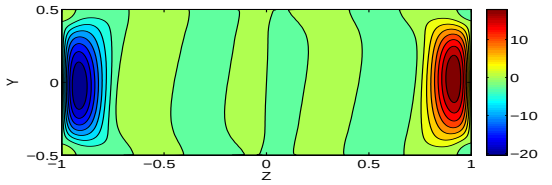

(b) $V(y, z)$

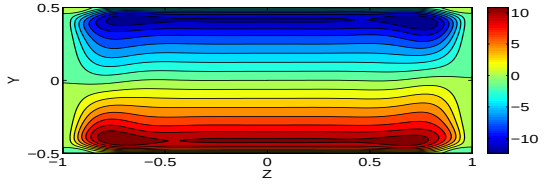

(c) $W(y, z)$

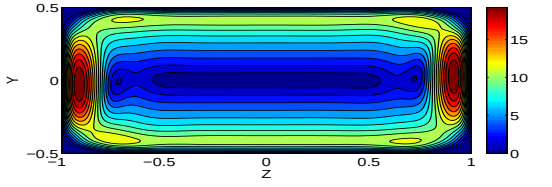

(d) $\sqrt{V^2 + W^2}$

FIGURE 4 – Velocity contours in the transverse (y,z) plane at $x = 0$ for $Ta = 10^6$, $Pr = 10^{-3}$ and $Gr = 2.5 \times 10^4$.

As shown in Fig. 4 by the velocity contours obtained for $Ta = 10^6$, the resulting asymptotic flow is composed of two longitudinal rolls concentrated near the front and back lateral walls, in places where the initial velocity was weak due to adherence effect, implying weak effect of rotation. These longitudinal flows are fed by a transverse circulation occurring throughout the core region. In the region of ascent and descent of the longitudinal flow (at the hot and cold walls), the rotation promotes the flow through the longitudinal loop that is on the right when the flow approaches the considered wall. This figure (Fig. 4d) shows also (through the norm of the components contained in the transverse plane located at $x = 0$ ($V(y, z)$ and $W(y, z)$)) that the mean principal longitudinal loop is now rather changed to transverse loops.

3.2 Lagrangian description

An other way to describe the flow is the Lagrangian description. In order to analyze the effect of the rotation on the trajectories of fluid particles, a Lagrangian tracking is computed through the expression

$$\vec{X}(t) = \vec{X}_0 + \int_{t=0}^{t=n\times\Delta t} \vec{V} dt$$

where $n = 5 \times 10^5$ and $\Delta t = 0.01$, $\vec{X}_0$ is the initial position at $t = 0$ of the particle we track, $\vec{V}$ is the

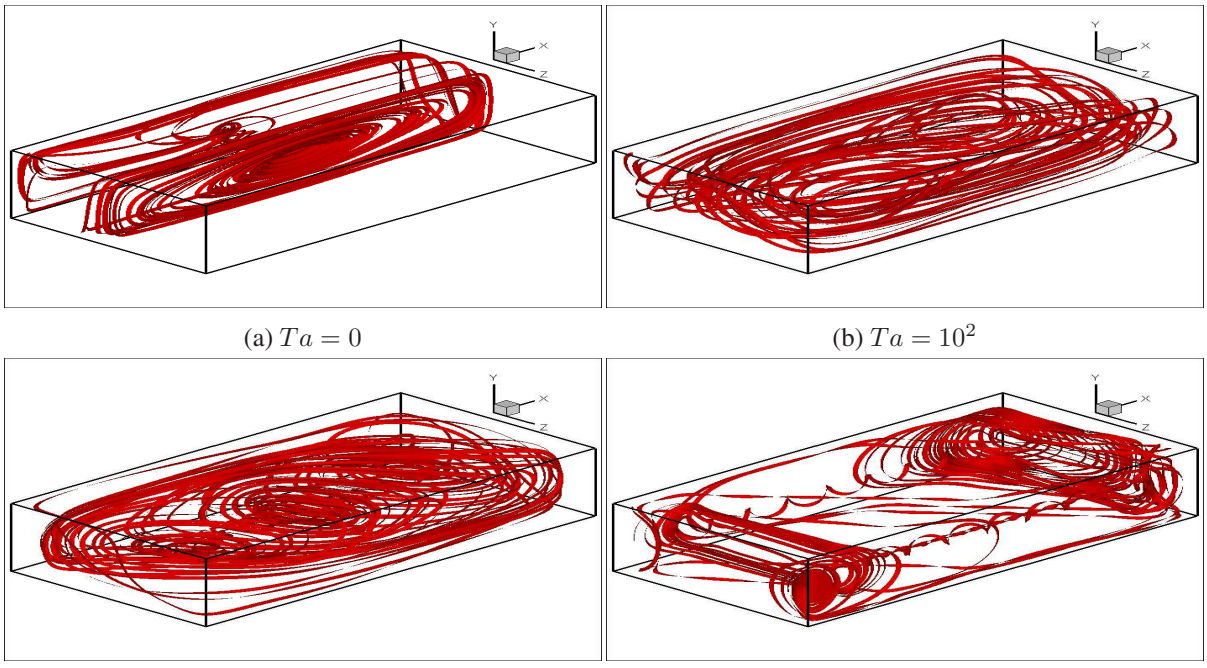

(a) $Ta = 0$ (b) $Ta = 10^2$

(c) $Ta = 10^4$ (d) $Ta = 10^6$

FIGURE 5 – Particle tracks issued from the point ($x = -1.9$, $y = 0.45$, $z = -0.9$) for different Taylor numbers, $Pr = 10^{-3}$ and $Gr = 2.5 \times 10^4$.

velocity field and $t = n \times \Delta t$ is the observation time. In the results presented in Fig. 5, the fluid particle is initially located at the position $\vec{X}_0(x = -1.9, y = 0.45, z = -0.9)$. For Ta=0 (Fig. 5a), we observe the motion described by Henry and Buffat [14]. It consists in a spiral motion in the two regions separated by the longitudinal vertical plane passing through the center of the cavity ; a particle near the edge makes a spiral motion of increasing radius when going towards the plane of symmetry ; it does not cross it and quickly returns to the edge of the cavity. When the cavity is submitted to a moderate rotation ($Ta = 10^2$

and $Ta = 10^4$), we observe the same kind of spiral path (Figs. 5b and 5c) but oriented with respect to a diagonal plane instead of the longitudinal central plane. This resulting structure is due to the fact that the rotation shifts the trajectories to the right. If we further increase the Taylor number ($Ta = 10^6$) and consequently the effect of rotation, we observe longitudinal paths along the front and back lateral walls, which acknowledge the existence of two longitudinal rolls in these places, and transverse to oblique paths in the core, which connect these longitudinal circulations (Fig. 5d).

3.3 Toward a simplified model

In the results presented above, we showed clearly the creation of transverse velocities in the cavity. We seek here to derive a simplified model which will be valid in the core region when the cavity is large enough.

We consider a cavity whose length L and width l are very large in comparison to its height h ($L >> h$ and $l >> h$) and which is submitted to a horizontal gradient of temperature. We also assume that there exist vertical boundaries located at $(x, z) = \pm\infty$ which allow the flow to return. In such a situation, a steady parallel flow solution depending only on the vertical y coordinate can be derived. The mean hypothesis that we are making here is that the velocity field is composed of two components: $U(y)$ the longitudinal flow originally forced by the applied temperature gradient and $W(y)$ the transverse component created by the Coriolis force and which must be equal to zero in the case of non-rotating situation. The temperature profile is given by $T(x, y) = x + \Theta(y)$.

Under these assumptions and by taking the curl of the momentum balance, equations (1), (2) and (3) are reduced to two coupled ODEs of third order for $U(y)$ and $W(y)$, which can be solved by introducing a complex velocity profile $\psi(y) = U(y) + i\,W(y)$ (BCs: $\psi(y = \pm 1/2) = \psi(y = 0) = 0$). It follows that $\psi(y)$ satisfies

$$\left(\frac{d^3}{dy^3} + i\sqrt{Ta}\frac{d}{dy}\right)\psi(y) = Gr. \tag{4}$$

We finally obtain

$$\psi(y) = \frac{i\,Gr}{2\sqrt{Ta}}\left(\frac{\sinh\left(\frac{(i-1)\sqrt[4]{Ta}}{\sqrt{2}}y\right)}{\sinh\left(\frac{(i-1)\sqrt[4]{Ta}}{2\sqrt{2}}\right)} - 2y\right) \tag{5}$$

The complex velocity profile (5) obtained herein is known in Russian literature also (see Chekulaev & Svarts [20], for example). The velocity components are obtained by separating the real and the imaginary parts of (5), i.e. $U(y) = \mathcal{R}e\,[\psi(y)]$ and $W(y) = \mathcal{I}m\,[\psi(y)]$. Note that

$$\psi(y) \sim Gr\left(\tfrac{y^3}{6} - \tfrac{y}{24}\right) \quad \text{as} \quad Ta \to 0,$$

which is the well-known cubical Hadley profile [19].

We present in Fig. 6 a comparison between the analytic profiles presented in solid lines and the 3D numerical results plotted with circles. We have plotted $u(y) = U(y)/Gr$ and $w(y) = W(y)/Gr$. The numerical results have been computed for $Gr = 10^3$. We see that the comparison is very good, showing that the 1D approximation proposed by the simplified model is meaningful for the flow in the central zone of sufficiently large 3D cavities.

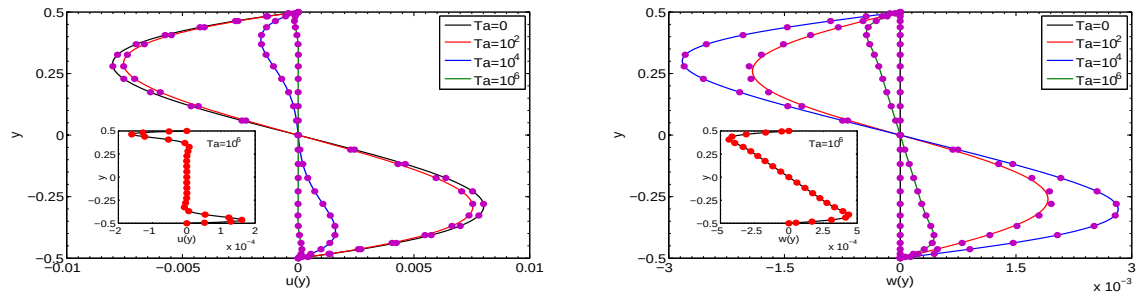

FIGURE 6 – Effect of the Taylor number on: (a) the longitudinal velocity profile $u(y) = U(y)/Gr$ and (b) the transverse velocity profile $w(y) = W(y)/Gr$ at $y = z = 0$.

4 Conclusion

This study considered the effect of rotation on convection in a differentially heated cavity. The increase of the Taylor number was found to induce significant modifications of the flow intensity and structure.

The rotation induces a decrease of the convective flow intensity, due to the decrease of the main longitudinal flow. This decrease is associated with an increase of the transverse velocity component, which was initially weak in the convective flow. This transfer of energy between the horizontal velocity components is connected with the Coriolis force and the deviation of the velocity components it induces: a longitudinal component creates a transverse component, which, in turn, induces a longitudinal component opposite to the initial one.

At large Taylor numbers, all the velocity components will eventually decrease with asymptotic variations. The global structure of the convective flow is also changed under rotation. Breakings of symmetry occur and only the symmetry with respect to the center of the cavity is preserved. The simple one-roll flow occupying the whole cavity is gradually modified when rotation is applied, with concentration of the longitudinal flow in specific zones and increased importance of the transverse circulation.

In the asymptotic state, the flow consists of two longitudinal rolls, located close to the front and back lateral walls, and a strong exchange between these two rolls through transverse circulation loops.

Références

[1] G. Dhanaraj, K. Byrappa, V. Prasad and M. Dudley, Springer Handbook of Crystal Growth, Springer-Verlag Berlin Heidelberg, 2010.

[2] D. Henry and H. Ben Hadid, Multiple flow transitions in a box heated from the side in low-Prandtl-number fluids, Phys. Rev. E, 76 (2007) 016314.

[3] M. Lappa, Secondary and oscillatory gravitational instabilities in canonical three-dimensional models of crystal growth from the melt. Part 2: lateral heating and the Hadley circulation, C. R. Mécanique, 335 (2007) 261-268.

[4] P. Laure and B. Roux, Linear and non-linear analysis of the Hadley circulation, J. of Crystal Growth, 97 (1989) 226-234.

[5] T. P. Lyubimova, D. V. Lyubimov, V. A. Morozov, R. V. Scuridina, H. Ben Hadid and D. Henry, Stability of convection in a horizontal channel subjected to a longitudinal temperature gradient. Part 1. Effect of aspect ratio and Prandtl number, J. Fluid Mech., 635 (2009), 275-295.

[6] G. S. Hadley, Concerning the cause of the general trade winds, Phil. Trans., 29 (1735) 58-62.

[7] D. Fultz, Experimental analogies to atmospheric motions, Compendium of meteorology, (1951).

[8] M. Ghil, P. Read and L. Smith, Geophysical flows as dynamical systems: the influence of Hide's experiments, Astronomy & Geophysics, 51 (2010) 4.28-4.35.

[9] R. Hide, A path to discovery in geophysical fluid dynamics, Astronomy & Geophysics, 51 (2010) 4.16-4.23.

[10] D. T. Hurle E. Jakeman and C. P. Johnson, Convective temperature oscillations in molten gallium, J. Fluid Mech., 64 (1974) 565-576.

[11] B. Hof, A. Juel and T. Mullin, Magnetohydrodynamic damping of oscillations in low Prandtl number convection, J. Fluid Mech., 545 (2005) 193-201.

[12] H. Ben Hadid, D. Henry and S. Kaddeche, Numerical study of convection in the horizontal Bridgman configuration under the action of a constant magnetic field. Part 1: two dimensional flow, J. Fluid Mech., 333 (1997) 23-56.

[13] H. Ben Hadid and D. Henry, Numerical study of convection in the horizontal Bridgman configuration under the action of a constant magnetic field. Part 2: three dimensional flow, J. Fluid Mech., 333 (1997) 57-83.

[14] D. Henry and M. Buffat, Two and three dimensional numerical simulations of the transition to oscillatory convection in low Prandtl fluids, J. Fluid Mech., 374 (1998) 145-171.

[15] B. Xu, B. Q. Li and D. E. Stock, An experimental study of thermally induced convection of molten gallium in magnetic fields, Int. J. Heat Mass Transfer, 49 (2006) 2009-2019.

[16] W. Dridi, D. Henry and H. Ben Hadid, Influence of acoustic streaming on the stability of a laterally heated three dimensional cavity, Phys. Rev. E, 77 (2008) 046311.

[17] G. E. Karniadakis, High-order splitting methods for incompressible Navier-Stokes equations, J. Comp. Physics, 97 (1991) 414-443.

[18] A. El Gallaf, Etude de la dynamique non-linéaire des écoulements chauffés et soumis à des champs magnétiques, Thèse de doctorat, Ecole Centrale de Lyon, 2010.

[19] J. E. Hart, Stability of thin non-rotating Hadley circulations, J. Atmos. Sci., 29 (1972) 687-696.

[20] D. G. Chikulaev and K. G. Shvarts, Effect of rotation on the stability of advective flow in a horizontal liquid layer with solid boundaries at small Prandtl numbers, Fluid Dynamics, 50 (2015) 215-222.